

# Excess dissipation in a single-electron box: The Sisyphus resistance

F. Persson,\* C.M. Wilson, M. Sandberg, G. Johansson, and P. Delsing†

*Department of Microtechnology and Nanoscience (MC2),  
Chalmers University of Technology, SE-412 96 Göteborg, Sweden*

(Dated: November 2, 2018)

We present measurements of the ac response of a single-electron box (SEB). We apply an rf signal with a frequency larger than the tunneling rate and drive the system out of equilibrium. We observe much more dissipation in the SEB than one would expect from a simple circuit model. We can explain this in terms of a mechanism that we call the Sisyphus resistance. The Sisyphus resistance has a strong gate dependence which can be used for electrometry applications.

Dissipation in quantum systems has been an important area of research for many years. It has lately gained renewed attention as quantum systems have increasingly come to the forefront of technology, including research in nanotechnology and quantum information. In many of these contexts, dissipation can be modeled using a simple two-level system (TLS) or an ensemble of them. It is therefore generally useful to study dissipation in TLSs. For instance, in the context of quantum information [1], where any dissipation causes unwanted decoherence, TLSs are important in several different ways. First, the basic building block of all quantum bits is an effective TLS. In addition, the presence of parasitic TLSs in dielectrics has been shown to result in losses which degrade the quality factor of electrical resonators and limit the coherence of superconducting qubits [2]. Fast driving of a TLS through an avoided level crossings (ALC) recently received considerable attention, and has been analyzed in terms of Landau-Zener (LZ) transitions [3–5] and dressed states [6]. Recently, in a setup related to the one studied here, Sisyphus cooling [7] and amplification was observed in a superconducting circuit [8].

In this Letter, we study a mesoscopic circuit consisting of a small metallic island connected by a tunnel junction to a much larger reservoir. Charging effects (Coulomb blockade) result in well defined energy levels which become degenerate at a specific bias point. An ac drive is used to cyclically drive the system through this level crossing. Due to the low transparency of the tunnel barrier, the coupling between the levels is negligible and the probability of a LZ transition when crossing the degeneracy point is very close to unity. However, due to the large degeneracy of the electronic states on the island, the total system can have a significant relaxation (or tunneling) rate. If the frequency of the drive is comparable to the relaxation rate of the system, alternating excitation and relaxation of the system lead to excess dissipation which can be directly measured. We call this process the Sisyphus resistance. We develop a quantitative model of the behavior that shows very good agreement with the measured response.

The charging effects which give rise to the quantization of the energy levels have a very peculiar effect on dissipation in the circuit. Far away from the degeneracy point, the Coulomb blockade prevents tunneling, and results in a high Sisyphus resistance and low dissipation. However, at the degeneracy point, the charging effects result in a low Sisyphus resistance with dissipation much larger than that expected from a gate capacitance in series with an Ohmic resistor with the value of the tunneling resistance, Fig. 1c. We note that the Sisyphus mechanism described here is not limited to Coulomb blockade devices, but should be a generic property of any system with an energy level crossing. In an analogous way to the Sisyphus mechanism discussed here, it was suggested that phonon pumping of TLSs can dominate losses in micro-mechanical resonators at low temperatures [9] and one could imagine having the same effect in electrical resonators. It has been suggested that TLSs may dominate the loss in electrical resonators under conditions important for quantum information applications [2].

The circuit of interest in this Letter is very similar to the radio-frequency (rf) SET [10] except that the SET is replaced by a single-electron box (SEB) (see Fig. 1a). The SEB consists of an aluminum island connected by a tunnel junction to a charge reservoir and three different capacitive gates. There is an rf gate which couples the SEB to an on-chip lumped-element resonator. The SEB also has a dc gate to adjust the static potential of the island and a microwave (mw) gate used for spectroscopic characterization of the SEB. We perform rf reflectometry measurements by sending a continuous rf signal to the device. On resonance, the rf signal will excite the resonator, which in turn will drive the potential of the SEB island around the working point set by the dc gate. Depending on the dissipation in the resonator caused by the SEB, the magnitude of the reflected signal will change. We measure both the magnitude and phase of the reflected signal to characterize this dissipation.

To explain the observed dissipation, we can consider the two energy levels,  $E_0$  and  $E_1$ , in Fig. 1d. The energy of each level can be controlled by the parameter  $n_g$ , the normalized gate voltage in units of induced electrons. At the degeneracy point,  $n_g = 0.5$ , the two levels cross. Let us now assume that the system is biased at a point  $n_g^0$  and driven around this point by a fast rf drive of amplitude  $\delta n_g$ . We imagine following the system through one cycle

\*fredrik.persson@chalmers.se

†per.delsing@chalmers.se

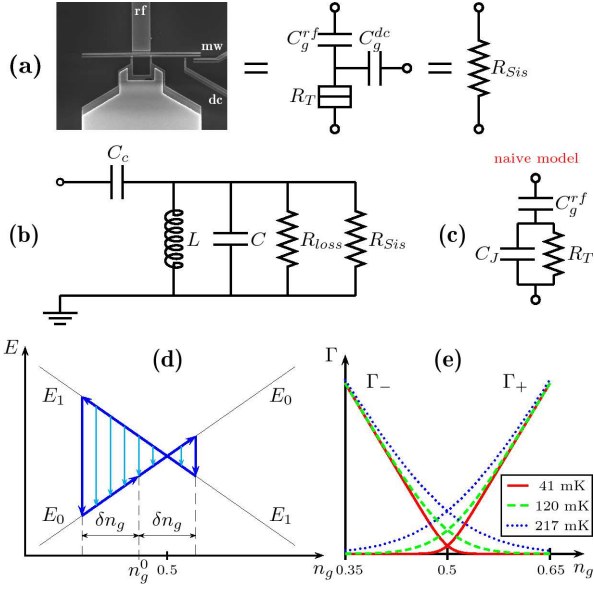


FIG. 1: (a) A scanning-electron micrograph of the SEB. The island of the SEB is  $8 \mu\text{m}$  long and  $100 \text{ nm}$  wide. The SEB has three different gates: one rf gate connecting the SEB to a parallel resonator used for readout, one dc gate to set the working point and one microwave gate used in the characterization. To the right of the micrograph are different circuit models used in the discussion of the measured response. (b) The circuit model used in analyzing the response. The SEB is modeled by the voltage dependent resistor  $R_{Sis}$ . The internal losses in the resonator, mostly due to the normal top layer, are modeled as a parallel resistor  $R_{loss}$ . The coupling capacitor  $C_c$  is used to decouple the resonator from the  $50 \Omega$  impedance of the environment and thereby increase the quality factor of the resonator. (c) A naive model of the SEB, which is compared with the Sisyphus resistance in the text.  $C_J$  is the geometric capacitance of the tunnel junction. (d) The process behind the Sisyphus resistance.  $E_0$  and  $E_1$  are the electrostatic energies of the two charge states. Starting from a charge state of lower energy, the rf signal  $\delta n_g$  drives the system past the degeneracy point and into an excited state, at the same time charging the system. When the system eventually relaxes by tunneling, the charging energy is lost. (e) The tunnel rates between the two charge states as a function of the normalized gate voltage,  $n_g$ , for three different temperatures.

of the rf drive (see Fig. 1d). In the first half cycle, we start on the left (right) side of the degeneracy point in the ground state. Moving across the degeneracy point at a high rate the system stays in the same state, which becomes the excited state. As we move away from the degeneracy point, the tunneling rate,  $\Gamma_{+(-)}$ , for electrons on to (off from) the island, increases (see Fig. 1e) until a tunneling event occurs. The energy that had been put into the system is now dissipated and we have to start over again in the second half cycle. In contrast, when we are far from degeneracy the energy put into the system during the first half cycle is given back during the second.

The electrostatic energy of the SEB is  $E = E_C(n - n_g)^2$  where  $n$  is the number of electrons added to the is-

land from its neutral state and  $n_g$  is the charge induced on the gate capacitance by the external voltage. Here  $E_C = e^2/2C_\Sigma$  is the charging energy and  $C_\Sigma$  is the total capacitance of the SEB island. For low enough temperature,  $k_B T \ll E_C$ , and a gate charge ranging between 0 and 1, only two charge states ( $E_0$  and  $E_1$ ) need to be considered. The dynamics of the driven SEB is then governed by the following master equation (ME)

$$\dot{P}_0 = \Gamma_- P_1 - \Gamma_+ P_0 \quad (1a)$$

$$\dot{P}_1 = \Gamma_+ P_0 - \Gamma_- P_1 \quad (1b)$$

where  $P_0$  and  $P_1$  are the probabilities of being in the two charge states and the tunneling rates are given by the orthodox theory for single-electron tunneling [11]

$$\Gamma_\pm = \frac{\mp \Delta E / h}{1 - e^{\pm \Delta E / k_B T}} \frac{R_K}{R_T} \quad (2)$$

and where  $\Delta E = E_1 - E_0 = E_C(1 - 2n_g(t))$ ,  $n_g(t) = n_g^0 + \delta n_g \sin(\omega_0 t)$  and  $\omega_0 = 2\pi f_0$  is the angular frequency of the rf drive. Here  $n_g^0 = C_g^{dc} V_g / e$  is the dc gate charge,  $R_K = h/e^2$  is the resistance quantum and  $R_T$  the tunneling resistance of the junction in the SEB. The normalized rf amplitude is  $\delta n_g = C_g^{rf} V_g^{rf} / e$ , where  $V_g^{rf}$  is the voltage amplitude inside the resonator. In order to solve the ME, we expand the tunneling rates (2) around the working point,  $n_g^0$ , to first order in  $\delta n_g$  and insert them into the ME. We then linearize the equation to get a first order linear differential equation for  $P_1$  (or  $P_0$ ) that can be solved analytically to get  $P_0(t)$  and  $P_1(t)$ . The average power dissipation, *i.e.* the energy transferred to the bath per cycle of the rf drive,  $T = 1/f_0$ , can then be calculated as

$$P_{Sis} = \frac{1}{T} \int_0^T dt [P_1 \Gamma_- \Delta E - P_0 \Gamma_+ \Delta E] \quad (3)$$

For a resistor,  $R$ , driven by an AC-voltage,  $\delta V$ , the average power dissipation is  $P = \delta V^2 / 2R$ . By comparing these two values we can define the Sisyphus resistance of the SEB,

$$R_{Sis} = 2R_T \left( \frac{C_\Sigma}{C_g^{rf}} \right)^2 \frac{k_B T}{\Delta E^0} \sinh \left( \frac{\Delta E^0}{k_B T} \right) \left( 1 + \frac{\gamma^2}{\omega_0^2} \right) \quad (4)$$

where  $\Delta E^0 = E_C(1 - 2n_g^0)$  is the energy splitting at the working point and  $\gamma = \Gamma_+ + \Gamma_- = \frac{\Delta E^0}{h} \frac{R_K}{R_T} \coth \left( \frac{\Delta E^0}{2k_B T} \right)$  is the equilibration rate of the system. This expression is only valid for  $\delta n_g \lesssim k_B T / E_C$  where the linear expansion of the tunneling rates is a good approximation. In this limit of small amplitudes, the Sisyphus resistance is independent of the actual amplitude. In addition to the Sisyphus resistance, the impedance of the SEB can also have a reactive component. However, our theoretical estimates predict that the gate dependence of this reactance is negligible in our experiment.

The device was fabricated in a multilayer process. Starting from a high-resistivity silicon wafer with a native oxide, the wafer was first cleaned using rf back sputtering directly after which a 60 nm thick layer of niobium was sputtered. To pattern the niobium, we used an Al mask made by e-beam lithography and e-beam evaporation. The niobium was then etched in a CF<sub>4</sub> plasma to form the inductor and bottom plates of the capacitors (see Fig. 1a). The Al mask was removed with a wet-etch based on phosphoric acid. Using PE-CVD, we then deposited an insulating layer of 200 nm of silicon nitride which covers the whole wafer; connections to the niobium layer were only made through capacitors. After using a combination of DUV photolithography to define bonding pads along with e-beam lithography to define the top layer of the capacitors, a 3/80/10 nm thick layer of Ti/Au/Pd was deposited by e-beam evaporation. Finally, the layer containing the SEB was made by e-beam lithography and two-angle shadow evaporation of 30+50 nm of aluminum, with 6 min of oxidation at 4 mbar.

The device was cooled in a dilution refrigerator with a base temperature of about 20 mK. For the readout, we used an Aeroflex 3020 signal generator to produce the rf signal. The signal was heavily attenuated and filtered and was fed to the tank circuit via two Pamtech circulators positioned at the mixing chamber. The reflected signal was amplified by a Quinstar amplifier at 4K with a nominal noise temperature of 1 K. The in-phase and quadrature component of the signal were finally measured using an Aeroflex 3030 vector digitizer.

In order to determine various device parameters, we performed dressed-state spectroscopy of the box in the superconducting state [6]. The quantum capacitance of the box was used for readout [12, 13]. In order to determine the charging energy, we applied microwave frequencies of  $f_\mu = 10\text{-}11$  GHz to the mw gate while slowly sweeping the dc-gate. Multiphoton resonances occur when  $mhf_\mu \approx 4E_C(1 - n_g)$ . From the positions of the multiphoton resonances, we can determine the charging energy [6]. For this device,  $E_C/h = 15.0 \pm 0.1$  GHz which corresponds to a total capacitance of  $C_\Sigma = 1.29$  fF for the SEB. Using this value of  $E_C$ , we then extracted a value for the Josephson coupling energy of  $E_J/h = 3.6 \pm 0.2$  GHz from conventional spectroscopy.

For the normal state measurements, we applied a parallel magnetic field of 600 mT in order to suppress superconductivity in the Al but not in the Nb. The resonator circuit was first characterized by measuring the reflection coefficient,  $S_{11}$ , as a function of frequency. Fitting the real and imaginary part of  $S_{11}$  simultaneously, the parameters of the resonator could be determined. From the fit we extracted  $L = 322$  nH,  $C_c = 92.1$  fF,  $C = 109.5$  fF and  $R_{loss} = 608$  k $\Omega$ . This corresponds to a resonant frequency of  $f_0 = 624.7$  MHz and a total Q-value of 97. The total Q-value has contributions both from the coupling to the external impedance of  $R_0 = 50$   $\Omega$ ,  $Q_0 = (C + C_c)/C_c^2\omega_0^2 R_0 = 121$ , and from internal losses,  $Q_R = \omega_0 R(C + C_c)$ , where  $R = R_{loss}R_{Sis}/(R_{loss} + R_{Sis})$ .

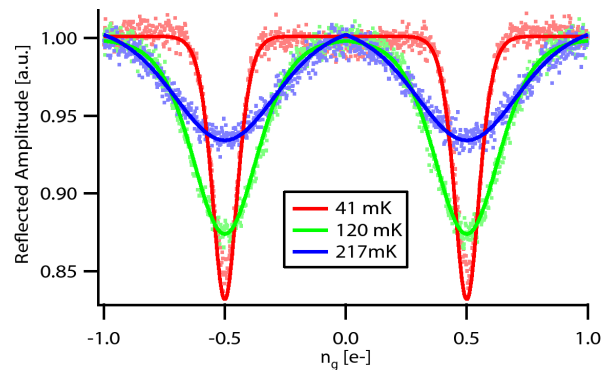


FIG. 2: The reflected amplitude, for low rf amplitudes ( $\delta n_g \approx 0.04$ ), as a function of the bias point,  $n_g$ , for three different temperatures. The theory (solid lines) are fit to the measured data (dots) using the analytic formula for the Sisyphus resistance, (4), inserted into the expression for the reflection coefficient of the combined system.

Away from the degeneracy point, where  $R = R_{loss}$ , we find  $Q_R = 481$ . The main contribution to the internal loss, which we represent by  $R_{loss}$ , is probably due to the top layer of the capacitors which was made out of gold. For similar circuits with superconducting Al as the top layer, we see much less internal loss.

Measurements of the ac-response were performed by slowly sweeping the dc-gate and continuously monitoring  $S_{11}$  at the fixed frequency  $f_0$ . There was little or no change in the phase of  $S_{11}$  but there was a substantial reduction in its magnitude when the SEB was close to its degeneracy points at  $n_g = \pm 0.5$ . The measurements were done for a range of temperatures and rf amplitudes. In Fig. 2, the measured response is shown for three different temperatures as a function of the dc-gate charge. Here we used a low enough amplitude ( $\delta n_g \approx 0.04$ ) that the observed response was amplitude independent. The measured data were then fit to theory by replacing the SEB by its Sisyphus resistance using (4) and calculating the reflection coefficient for the combined system at resonance,

$$S_{11}(\omega_0) = \frac{Z_L(\omega_0) - R_0}{Z_L(\omega_0) + R_0} = \frac{k(Q_0 - Q_R) - i}{k(Q_0 + Q_R) + i},$$

$$Z_L(\omega_0) = \frac{1}{j\omega_0 C_c + \omega_0^2 C_c^2 R}, \quad (5)$$

where  $Z_L(\omega_0)$  is the impedance on resonance of the total load, as pictured in Fig. 1b, and  $k = C_c/(C + C_c)$ . The two fitting parameters were  $R_T$  and  $C_g^{rf}$ , which we were not able to determine by independent measurements. The two higher temperature curves were fit simultaneously, giving  $R_T = 49$  k $\Omega$  and  $C_g^{rf} = 0.31$  fF. The extracted value of  $R_T$  agrees with the measured value of  $E_J$  within the experimental error. The last curve was then fit by adjusting only the temperature, yielding an electron base temperature of  $T = 41$  mK.

We see that at the degeneracy point we get roughly

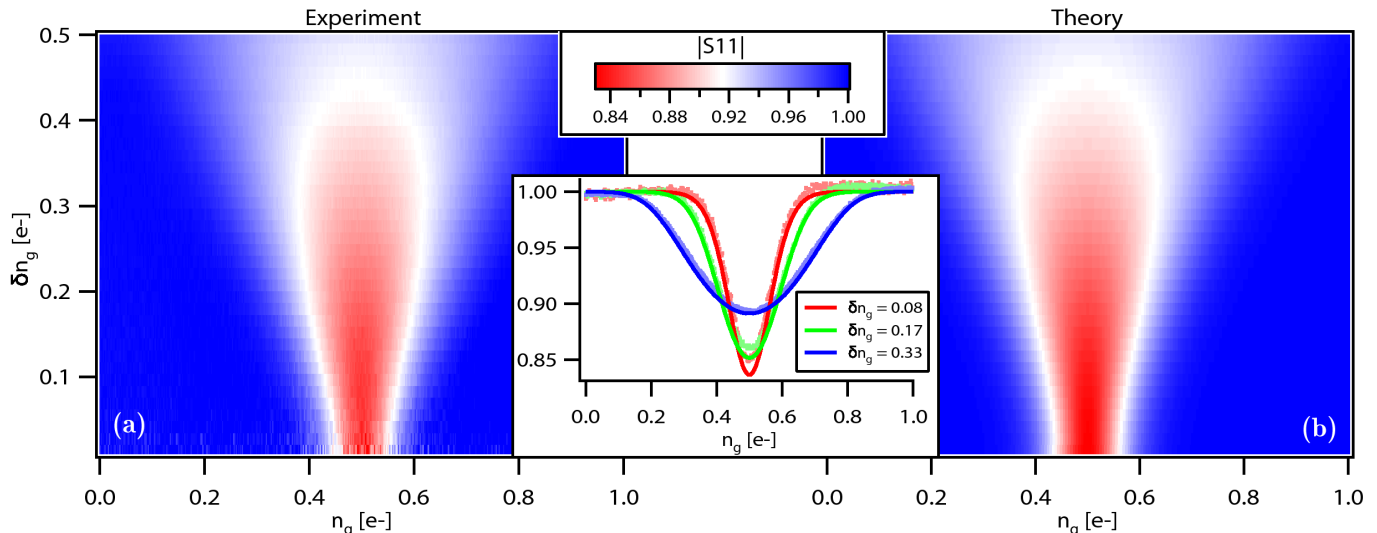


FIG. 3: The normalized reflected amplitude,  $|S_{11}|$ , measured at the base temperature, as a function of the bias point,  $n_g^0$ , and the rf amplitude,  $\delta n_g$ . In (a) are the measured data and in (b) is the calculated response, obtained by numerically solving the full ME. The only adjustable parameter is the total rf coupling, which sets the y-scale. In the inset, we show three line cuts comparing the measured (dots) and calculated response (solid lines). We see a very good agreement between theory and data.

17% absorption. This is a factor of eight more than the 2% that is expected from the naive circuit model shown in Fig. 1c. If we compare the dissipated power due to the Sisyphus resistance,  $P_{Sis}$  (Eq. (3)), to the dissipation, expected from this naive circuit model,  $P_{cir}$ , we get that  $P_{Sis}/P_{cir} = \frac{1}{2} (1 + (\omega_0 R_T C_\Sigma)^2) / ((k_B T / E_C)^2 + (\omega_0 R_T C_\Sigma)^2) \sim 8$ . A simple way to understand the large discrepancy is to consider the voltage that develops over the tunnel junction in the two cases. In between tunneling events, the effective resistance of the blockaded junction is much higher than  $RT$ . Thus, the typical voltage developed across the blockaded junction is much larger than would develop across a junction that is not blockaded. The typical energy scale of the dissipative tunneling events is therefore larger. This leads to the curious result that, due to the Sisyphus effect, the dissipation in the SEB is actually significantly *increased* by the Coulomb blockade, which is the opposite of what is typically found in single-electron devices. At the degeneracy point, there is a small discrepancy between the data and theory at the lowest temperatures. This could possibly be explained by temperature dependent renormalization effects [14].

Using the parameters extracted from the measurements in Fig. 2, we can then calculate the response for arbitrary  $\delta n_g$  and  $T$ . In Fig. 3, we show the measured response at the base temperature as a function of  $\delta n_g$  together with the calculated response, obtained by numerically solving the full ME. The only additional fitting parameter is the total rf coupling, which sets the y-scale of the data. We see a very good agreement between experiment and theory.

Since the Sisyphus resistance has such a strong gate dependence, it is possible to use it as the basis for a

very sensitive electrometer. If the SEB is biased on the side of the degeneracy point where the response has the maximum slope, a small variation in the gate charge will give a large change in the magnitude of the reflection coefficient. We have estimated the sensitivity,  $\delta Q = e(\delta V / V) |\partial S_{11} / \partial n_g|^{-1}$  where  $V$  and  $\delta V$  are the applied signal and noise voltage at the input of the amplifier, respectively. We calculate  $\delta V$  by assuming a system noise temperature of 1.5 K due to noise added by the amplifiers and the insertion loss between the sample and the first amplifier. We used the calculated response in Fig. 3 to calculate the transfer coefficient,  $\delta |S_{11}| / \delta n_g$ , as a function of rf amplitude. We get a best sensitivity of  $74 \mu e / \sqrt{\text{Hz}}$ . This is not too far from the best measured sensitivity which we obtained:  $86 \mu e / \sqrt{\text{Hz}}$ . In order to optimize the sensitivity, as a first approximation, we maximize the transfer coefficient  $|\partial S_{11} / \partial n_g|$  using Eq. (5) and the analytical expression (4). If we use an applied voltage corresponding to  $\delta n_g = k_B T / E_C$  we get that

$$\delta Q(n_g^0) = \frac{k C_g^{rf} \delta V}{\sqrt{2}} Q_R (Q_0 + Q_R) \left( \frac{\partial Q_R}{\partial x} \right)^{-1} \quad (6)$$

where  $R(n_g^0) = R_{loss} || R_{Sis}(n_g^0)$  and  $x(n_g^0) = \frac{\Delta E^0(n_g^0)}{k_B T}$ . Inserting the parameters for this sample results in a best sensitivity of  $117 \mu e / \sqrt{\text{Hz}}$ . Although there is a deviation from the numerical calculation, which can be attributed to a too low estimate of the optimal probe amplitude, the formula still give us valuable information on how to improve the sensitivity. By reducing the losses in the resonator to reach an internal Q-value of  $10^4$  (which we have obtained in similar resonator with a superconducting top layer) and by decreasing the coupling capacitance,  $C_c$ , and the junction capacitance,  $C_J$ , by a factor three each

we estimate that the sensitivity can be improved by an order of magnitude.

The use of an rf-SEB instead of the more common rf-SET has some advantages. First, it is a simpler circuit, requiring just one tunnel junction, which is beneficial in, for example, molecular electronics where junctions are very difficult to fabricate. In fact, in Ref. 15 the same mechanism of dissipation that has been discussed here was used to probe the potential inside nanostructures. The model for the response developed in this Letter could be used to understand and improve the response in such a system. The single tunnel junction also makes the rf-SEB insensitive to electrostatic discharges, since there is no dc path through the device. This makes the rf-SEB more suitable for applications in demanding envi-

ronments, such as for scanning probes [16].

In conclusion, we have measured the dissipation in a single-electron box driven by an rf signal. The observed dissipation is surprisingly large and cannot be explained by a simple circuit model. We explain this result using a master equation description of the Sisyphus resistance. We also demonstrate that this phenomenon can be used for electrometry.

We thank the members of the Quantum Device Physics and Applied Quantum Physics groups for useful discussions. The samples were made at the nanofabrication laboratory at Chalmers. The work was supported by the Swedish VR and SSF, the Wallenberg foundation, and by the EU under the project EuroSQIP.

- 
- [1] J. Clarke and F. K. Wilhelm, *Nature* **453**, 1031 (2008).
  - [2] J. M. Martinis, K. B. Cooper, R. McDermott, M. Steffen, M. Ansmann, K. D. Osborn, K. Cicak, S. Oh, D. P. Pappas, et al., *Physical Review Letters* **95**, 210503 (2005).
  - [3] A. V. Shytov, D. A. Ivanov., and M. V. Feigel'man, *Euro. Phys. J. B* **36**, 263 (2003).
  - [4] W. Oliver, Y. Yu, J. Lee, K. Berggren, and L. Levitov, *Science* **310**, 1653 (2005).
  - [5] M. Sillanpää, T. Lehtinen, A. Paila, and Y. Makhlin, *Phys. Rev. Lett.* **96**, 187002 (2006).
  - [6] C. M. Wilson, T. Duty, F. Persson, M. Sandberg, G. Johansson, and P. Delsing, *Phys. Rev. Lett.* **98**, 257003 (2007).
  - [7] D. J. Wineland, J. Dalibard, and C. Cohen-Tannoudji, *J. Opt. Soc. Am. B* **9**, 32 (1992).
  - [8] M. Grajcar, S. H. W. van der Ploeg, A. Izmalkov, E. Ilichev, H. G. Meyer, A. Fedorov, A. Shnirman, and G. Schon, *Nat Phys* **4**, 612 (2008).
  - [9] K. H. Ahn and P. Mohanty, *Phys. Rev. Lett.* **90**, 085504 (2003).
  - [10] R. J. Schoelkopf, P. Wahlgren, A. A. Kozhevnikov, P. Delsing, and D. E. Prober, *Science* **280**, 1238 (1998).
  - [11] D. V. Averin and K. K. Likharev, *Mesoscopic Phenomena in Solids* (Elsevier, Amsterdam, 1991).
  - [12] T. Duty, G. Johansson, K. Bladh, D. Gunnarsson, C. M. Wilson, and P. Delsing, *Phys. Rev. Lett.* **95**, 206807 (2005).
  - [13] G. Johansson, L. Tornberg, and C. M. Wilson, *Phys. Rev. B* **74**, 100504(R) (2006).
  - [14] Y. I. Rodionov, I. S. Burmistrov, and A. S. Ioselevich, *Phys. Rev. B* **80**, 035332 (2009).
  - [15] Z. Jun, M. Brink, and P. L. McEuen, *Nano Letters* **8**, 2399 (2008).
  - [16] H. T. A. Brenning, S. E. Kubatkin, D. Erts, S. G. Kafanov, T. Bauch, and P. Delsing, *Nano Letters* **6**, 937 (2006).